



# Soft computing techniques in prediction Cr(VI) removal efficiency of polymer inclusion membranes

Muhammad Yaqub<sup>1</sup>, Beytullah EREN<sup>2\*</sup>, Volkan Eyupoglu<sup>3</sup>

<sup>1</sup>Kumoh National Institute of Technology Gumi, Republic of Korea

<sup>2</sup>Department of Environmental Engineering, Sakarya University, Sakarya, Turkey

<sup>3</sup>Science Faculty, Chemistry Department, Cankiri Karatekin University, Cankiri, Turkey

## ABSTRACT

In this study soft computing techniques including, Artificial Neural Network (ANN) and Adaptive Neuro-Fuzzy Inference System (ANFIS) were investigated for the prediction of Cr(VI) transport efficiency by novel Polymer Inclusion Membranes (PIMs). Transport experiments carried out by varying parameters such as time, film thickness, carrier type, carrier rate, plasticizer type, and plasticizer rate. The predictive performance of ANN and ANFIS model was evaluated by using statistical performance criteria such as Root Mean Standard Error (RMSE), Mean Absolute Error (MAE), and Coefficient of Determination ( $R^2$ ). Moreover, Sensitivity Analysis (SA) was carried out to investigate the effect of each input on PIMs Cr(VI) removal efficiency. The proposed ANN model presented reliable and valid results, followed by ANFIS model results. RMSE and MAE values were 0.00556, 0.00163 for ANN and 0.00924, 0.00493 for ANFIS model in the prediction of Cr(VI) removal efficiency on testing data sets. The  $R^2$  values were 0.973 and 0.867 on testing data sets by ANN and ANFIS, respectively. Results show that the ANN-based prediction model performed better than ANFIS. SA demonstrated that time; film thickness; carrier type and plasticizer type are major operating parameters having 33.61%, 26.85%, 21.07% and 8.917% contribution, respectively.

**Keywords:** Adaptive neuro-fuzzy inference system, Artificial neural networks, Chromium, Removal efficiency, Sensitivity analysis

## 1. Introduction

Chromium is frequently encountered heavy metal in wastewaters due to its various industrial applications including textile dyeing, tanneries, metallurgy, metal electroplating and wood preserving [1, 2]. In the past, numerous studies including adsorption [3] coagulation-sedimentation, chemical precipitation [4], biosorption [5], ion exchange [6], reverse osmosis [7], electrodialysis [8], ion exchange-assisted membrane [9, 10], and electrochemical [11] techniques were conducted to combat heavy metals contamination issue. Recently, Polymer Inclusion Membranes (PIMs) process has been widely and successfully used for metal ion extraction, separation of inorganic species, biochemical and biomedical applications [12]. In extraction or separation based processes, a larger attention has been given to discover environmental friendly, portable and less toxic carrier or an organic solvents in the relevant literature. In last decades, anionic liquid (IL) based organic salts were accepted as potential molecules for extraction or separation purposes as

an alternative chemical family, which can replace traditional ones [13]. The simplicity, easy scale-up operation, less energy consumption, and environmental friendly characteristics proved liquid membranes a good alternate for heavy metals removal rather than conventional techniques.

Modeling is a valuable approach to develop a relation between parameters and efficiency to optimize and control the process for efficient design and operation. The development of a mathematical model for PIMs based separation process is a difficult task due to the non-linear, differential and complicated process. Due to outstanding characteristics in processing the non-linear relationships among variables in complex systems with reliable and robust results, Artificial Neural Networks (ANN) has been successfully employed in environmental engineering [14-17]. Another technique that integrates both neural networks and fuzzy logic principle has potential to capture the benefits of both in a single framework [18]. In the literature, the ANN model has been applied for evaluation of heavy metals removal through physic-chemical processes [19]



This is an Open Access article distributed under the terms of the Creative Commons Attribution Non-Commercial License (<http://creativecommons.org/licenses/by-nc/3.0/>) which permits unrestricted non-commercial use, distribution, and reproduction in any medium, provided the original work is properly cited.

Copyright © 2020 Korean Society of Environmental Engineers

Received March 4, 2019 Accepted June 13, 2019

\* Corresponding author

Email: beren@sakarya.edu.tr

Tel: +90 264 295 5642

ORCID: 0000-0001-6747-7004

from drinking water and from wastewater treatment systems [20, 21]. A comparative study of ANN to predict Cd removal efficiency of PIMs proved feed forward back-propagation and recurrent neural networks as best prediction models [22]. In other studies such as biosorption efficiency of *Zea Mays* for the removal of chromium from wastewater [23] and copper removal from aqueous solution by the ion-exchange process [24] was estimated by applying ANN modeling. The process optimization of Pb (II) and zinc (II) adsorption was studied by using ANN modeling techniques [25, 26]. ANN model was proposed to investigate copper removal from wastewater by adsorption on fungal biomass [27] and cadmium sorption by Shelled *Moringa Oleifera* Seed Powder from aqueous solution [28]. Moreover, ANN genetic algorithm and particle swarm optimization modeling was used for the prediction of copper removal from aqueous solutions by reduced graphene oxide-supported nanoscale zero-valent iron (nZVI/rGO) magnetic nanocomposites [29].

The Cr(VI) removal efficiency of PIMs cannot be determined by conventional mathematical techniques alone because of non-linear, differential and complicated process. Being a complicated process, the exact specification of the separation conditions involved in the process may lead to unreliable results in the practical applications. To improve the performance of PIMs, estimation, optimization, and analysis of the operating parameters should be accomplished by modeling and simulation, as well as, through laboratory experiments. Moreover, efficiency of PIMs to remove Cr(VI) has not been studied previously by applying soft computing techniques. Therefore, ANN and Adaptive Neuro-Fuzzy Inference System (ANFIS) models were considered for the prediction of PIMs Cr(VI) removal efficiency from aqueous solutions. The goal of this study is to propose the best soft computing technique in prediction Cr(VI) removal efficiency of PIMs from aqueous solution, and to optimize the process by considering the effect of various operational parameters through sensitivity analysis (SA) to check the acceptable conformity and individual effectiveness of each operating parameter.

## 2. Materials and Methodology

### 2.1. Experimental Design and Data Preparation

The experimental details were published as a separate study [30, 31]. The polymeric ionic membrane was prepared by using previous methods described in the literature [32, 33]. The Cr(VI) transport conditions were optimized by changing PIMs parameters; Cr(VI) transport time (the range is at 0-8 h), polymer membrane film thickness (the thickness range is in 25.17-151.24  $\mu\text{m}$ ), ionic liquid types as ion carrier (these are 1,3-dibutyl, 1,3-di hexyl, 1,3-di octyl, and 1,3-di decyl imidazolium bromide salts), carrier rate (the ranges is in 0-0.343, w/w), plasticizer type (2-nitrophenyl octyl ether; ONPOE, 2-nitrophenyl pentyl ether; 2-NPPE, bis(2-Ethylhexyl) adipate; B2EHA, tris(2-Ethylhexyl) phosphate; TEHP), plasticizer rate (the ranges is in 0-0.3377, w/w) versus the constant concentration and composition of feed (its composition is 25 mg/L Cr(VI) in 0.5  $\text{mol}\cdot\text{L}^{-1}$   $\text{H}_2\text{SO}_4$ ) and stripping (its composition is 2.0  $\text{mol}\cdot\text{L}^{-1}$  NaOH) phases, were investigated in previous experimental study [30, 31]. The experimental setup and its operation principle are presented

in Fig. S1. The data was collected from an experimental study regarding the selective transport of Cr(VI) through PVDF-HFP based PIMs containing symmetric imidazolium bromide salts as a carrier. 1,3-dibutyl, 1,3-di hexyl, 1,3-di octyl, and 1,3-di decyl imidazolium bromide salts substituted ionic liquids (ILs) synthesized and used in the production of PVDF-HFP based PIMs [30].

The experimental data for this study was obtained under different operating conditions such as time (ranges 0-8 h), film thickness of membrane (ranges 25.17-151.24  $\mu\text{m}$ ), carrier type range 1 to 4 (1-butyl, 2-decyl, 3-hexyl, and 4-octyl) and carrier rate (ranges 0-0.367 (w/w)), plasticizer type range 1 to 4 (1-TEHP, 2-NPPE, 3-B2EHA, and 4-ONPOE) and plasticizer rate (ranges 0-0.338 (w/w)) were used as inputs and removal efficiency of Cr(VI) (ranges 0.13-1.00 ( $C/C_0$ )) was used as output variable. Dataset is preprocessed before giving to the input layer. Some experimental data of operating parameters such as extractant type and plasticizer type were converted from characters to numerical data. Statistical information related to the data of each experiment is summarized in Table 1. The learning capacity of a model depends upon the size of training dataset as studied by [34]. Experimental data contained 460 rows was randomly divided into three groups for training (70%), validating (15%) and testing (15%) for both ANN and ANFIS.

**Table 1.** Data Statistics of Model Variables (n = 460)

Variables	Units	Data Statistics			
		$X_{\min}$	$X_{\max}$	$X_{\text{mean}}$	$\sigma$
<i>Input layer</i>					
Time	h	0.00	8.00	4.000	2.832
Carrier type(1 to 4)	-	1.00	4.00	2.826	1.167
Carrier rate	w/w	0.00	0.34	0.215	0.0679
Film thickness	$\mu\text{m}$	41.23	147.83	98.953	29.46
Plasticizer type (1 to 4)	-	1.00	4.00	3.673	0.809
Plasticizer rate	w/w	0.00	0.34	0.236	0.058
<i>Output layer</i>					
Removal efficiency	$C/C_0$	0.13	1.00	0.865	0.151

$X_{\min}$ ,  $X_{\max}$ ,  $X_{\text{mean}}$ : minimum, maximum and mean values,  $\sigma$ : standard deviation

### 2.2. Prediction Models

ANN and ANFIS models are evaluated in this study for their potential to predict Cr(VI) removal efficiency of PIMs. These approaches described briefly in the next sections. Neurosolution 6.0 used for the training and optimization of the ANN model while MATLAB was used for ANFIS modeling.

#### 2.2.1. ANN

ANN is a computational model based on the structure and functions of biological neural networks such as the human nervous system used for receiving, processing, and transmitting information regarding computer science [35]. ANNs are digitized models of human brain computer programs designed to simulate the way in which human brain processes information [36]. Generally, development of an ANN model consists of the following steps: data collection,

analysis and pre-processing of the data, creation, and configuration of the network, training, and validation of the network and finally simulations and predictions with the validated network [37]. The structure of ANN is comprised of an input layer, an output layer and one or more hidden layers as represented in Fig. S2 [32].

The primary component of ANN is the neuron also called "node." The inputs are represented by  $x_1, x_2, \dots, x_n$  and the output by  $Y$ . Feedforward back propagation learning technique is used in ANN because this technique error is processed by two steps; first is a feed-forward step where output of any node is computed by propagating the input value given from the input nodes and second is a backward step in which connection weights are amended by using error criteria [38]. ANN modeling consists of two stages including training and testing. Data modeling process divided into three parts mentioned as training, validation, and testing. In the first stage, the ANN model trained and validates on validation dataset in order to tune the algorithm parameters. During the testing phase, the proposed model used to test the performance of the trained network for unseen test data set.

Calculation of the output node is based on a weighted sum of the input signals from the proceeding neuron, changed by the transfer function (Fig. S2). The learning potential of a neuron is based on weight adjustment in conformity to reduce the error. The number of neurons in the input and output layer depends upon the number of input and output parameters, respectively. Although, selection of the number of neurons in a hidden layer is case dependent and significant decision in ANN modeling, generally, trial and error technique is applied to identify the best ANN architecture [39].

### 2.2.2. ANFIS

ANFIS is a combination of two soft-computing methods, ANN and fuzzy logic rules "If-Then" [40]. Fuzzy logic can change the qualitative aspects of human knowledge and insights into the process of precise quantitative analysis. An adaptive network is an example of a feedforward neural network with multiple layers. Additionally, the adaptive network has the architecture characteristics that consists of some adaptive nodes interconnected directly without any weight value between them. Each node in this network has different functions and tasks, and the output depends on the incoming signals and parameters that are available in the node. A learning rule that was used can affect the parameters in the node, and it can reduce the occurrence of errors at the output of the adaptive network [41]. FIS was built on the basic rules, where it consists of the selection of fuzzy logic rules "If-Then" as a function of the fuzzy set membership; and reasoning fuzzy inference techniques from basic rules to get the output. The basic rules can be constructed by an automatic generation or by an operator, where the searching rules are arranged by using input-output data numerically [42].

Jang *et al.* [40] conducted one of the first studies to develop architecture and a learning procedure for FIS by applying a neural network learning algorithm. Jang *et al.* [40] constructed a fuzzy set with if-then rules along with suitable membership functions (MFs) from the particular input-output pairs [40]. In ANFIS learning, membership function parameters are updated mainly by two techniques: (1) backpropagation for all parameters and (2) a hybrid method performing backpropagation for the parameters related to the input

membership and least-squares prediction for the parameters associated with output MFs [42]. Initially, a crisp input converted through the input MFs and the associated parameters to fuzzy input. Then, the fuzzy input processed through fuzzy rules to produce fuzzy output. After that, the fuzzy output was converted through the output MFs and the associated parameters to a crisp output as shown in Fig. S3 [43].

ANFIS working principle described by Ismail [44]. Fig. S4 shows the diagrammatic representation of the ANFIS algorithm. For illustration, supposed two inputs  $x$  and  $y$  and one output  $f$  in the FIS. Then the application of first-order Sugeno fuzzy model provided a typical rule set having two fuzzies if-then rules can articulate as:

Rule 1: If  $x$  is  $A_1$  and  $y$  is  $B_1$ ; then

$$f_1 = p_1x + q_1y + r_1 \quad (1)$$

Rule 2: If  $x$  is  $A_2$  and  $y$  is  $B_2$ ; then

$$f_2 = p_2x + q_2y + r_2 \quad (2)$$

In above equations  $x$  and  $y$  are input variables to the node  $i$ ,  $A_i, B_i$  are fuzzy sets which are characterized by convenient MFs and finally  $p_i, q_i$ , and  $r_i$  are the consequent parameters described in previous studies [40, 45, 46].

The function of the ANFIS model expressed as:

Layer 1: In this layer, every node produces membership grades for input parameter and node output  $O_{1,i}$  described by,

$$O_{1,i} = \mu A_i(x), \text{ for } i = 1, 2 \text{ or} \quad (3)$$

$$O_{1,i} = \mu B_{i-2}(y), \text{ for } i = 3, 4 \quad (4)$$

In these equations  $x$  (or  $y$ ) is the input to the node  $i$ ;  $A_i$  (or  $B_{i-2}$ ) is a line fuzzy linguistic-related to that node.  $O_{1,i}$  is this the grade of a fuzzy set, and it defines the degree to which the given input  $x$  (or  $y$ ) satisfies the quantifier. Different MFs selected including triangular, Gaussian, generalized bell-shaped and trapezoidal-shaped functions.

Layer 2: This layer shows that every node fixed node labeled as  $G$ , whose output is the product of all incoming signals:

$$O_{2,i} = w_i = \mu_{A_i}(x) \mu_{B_i}(y), \quad i = 1, 2 \quad (5)$$

Layer 3: The  $i_{th}$  node of this layer, labeled as  $N$ , computes the normalized firing strength as,

$$O_{3,i} = \bar{w}_i = \frac{w_i}{w_1 + w_2}, \quad i = 1, 2 \quad (6)$$

Layer 4: Every node  $i$  in this layer is an adaptive node with a node function,

$$O_{4,i} = \bar{w}_i f_i = \bar{w}_i (p_i x + q_i + r_i) \quad (7)$$

Here  $w_i$  is the output of layer 3, and  $\{p_i, q_i, r_i\}$  is the parameter set of this node.

Layer 5: In this single layer node is a fixed node which calculates the overall output as the summation of all entering signals [42, 47].

$$f = \text{Overall output}, t = O_{5,i} = \sum_i \bar{w}_i f_i = \frac{\sum_i w_i f_i}{\sum_i w_i} \quad (8)$$

### 2.3. Performance Evaluation

In this study, three performance measures used to evaluate models predicted results. The Root Mean Square Error (RMSE); Coefficient of Determination ( $R^2$ ); and the Mean Absolute Error (MAE) are common techniques as performance measures for evaluation of models [48]. These techniques described below:

- (1) The RMSE represents the error between model predictions and target values. It can be computed with Eq. (9) with a range from 0 to 1. Lower RMSE values are close to zero as preferable as there is no absolute criterion for a “good” value [49].

$$RMSE = \sqrt{\frac{\sum_{i=1}^n (Y_{obs}^i - X_{sim}^i)^2}{n}} \quad (9)$$

In this equation  $n$  represents the number of target values; and  $andare$  model predictions and their corresponding observed values, respectively.

- (2)  $R^2$  has estimated through Eq. (10). This value range between 0 and 1 (i.e., 0-100%) shows the percentage of variability between experimental data and model predictions.

$$R^2 = \left[ \frac{n \sum_{i=1}^n Y_{obs,i} Y_{sim,i} - (\sum_{i=1}^n Y_{obs,i})(\sum_{i=1}^n Y_{sim,i})}{\sqrt{[n \sum_{i=1}^n Y_{obs,i}^2 - (\sum_{i=1}^n Y_{obs,i})^2] \times [n \sum_{i=1}^n Y_{sim,i}^2 - (\sum_{i=1}^n Y_{sim,i})^2]}} \right]^2 \quad (10)$$

- (3) The MAE can be computed with Eq. (11) Moreover, its values can range from 0 to 1. Similar to RMSE, lower values of MAE indicate a good correlation between model predictions and experimental data [49].

$$MAE = \frac{1}{n} \sum_{i=1}^n |X_{sim}^i - Y_{obs}^i| \quad (11)$$

### 2.4. SA

SA was performed to identify the critical parameters and their degree of importance on the model outputs. SA is not only critical to model validation but also serves to guide future research efforts because it is a key to determine the more influential parameter in model development and providing information about the more sensitive parameters, which should be measured more accurately.

In order to measure the sensitivity of parameters three different techniques including plus one by one, leave one out and percentage contribution employed manually in this study. Plus one by one technique is performed by considering the first parameter initially

and then the continuous addition of the next parameter to confirm the best set of input parameter according to performance criteria. In leave one out technique, one input parameter removed in each run to demonstrate the individual contribution of that parameter. The leaving out of an essential parameter results in lower  $R^2$  and higher RMSE and MAE values indicating that the network is affected to a greater extent when that variable is excluded.

## 3. Results and Discussion

### 3.1. Pre-Assessment of Experimental Data

The experimental data were obtained by varying operating conditions such as time; film thickness; carrier type and carrier rate; plasticizer type; and plasticizer rate of PVDF-based PIMs for Cr(VI) removal [31]. The ranges of experimental parameters (independent variables) were as follows, film thickness of membrane 41.23 to 147.83  $\mu\text{m}$ ; time 0-8 h; carrier type 1-4 (1-butyl, 2-decyl, 3-hexyl, and 4-octyl imidazolium bromide salts) and carrier rate 0-0.343 (w/w); plasticizer type 1-4 (1-TEHP, 2-NPPE, 3-B2EHA, and 4-ONPOE); and plasticizer rate 0-0.3377 (w/w). Based on these ranges, the removal efficiency of Cr(VI) ranged as 0.13-1.00 (C/C<sub>0</sub>), which was the output variable. Statistical information related to the data of each experiment summarized in Table 1.

### 3.2. Modeling Results

#### 3.2.1. Determination of a suitable ANN model

In this study, to determine the optimum number of neurons in the hidden layer different topologies were investigated with changing neurons from 3 to 45 in hidden layer. Each topology repeated three times, and RMSE used as an error function. ANN model provided the best results by the Levenberg-Marquardt algorithm as previously studied [50] and Sigmoid Axon transfer function. By using trial and error method, it was noted that (6-15-1) is the best topology in this study as represented in Fig. S5. The optimal structure of ANN for the best prediction of PIMs Cr(VI) removal efficiency was observed by considering 6 variable input layer; 15 neurons in a hidden layer; and one variable output layer (6-15-1). Fig. 1 shows the proposed neural network architecture.

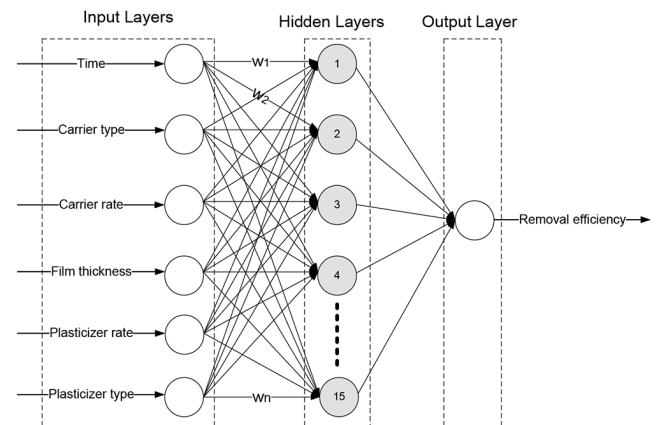


Fig. 1. Optimum structure of ANN model.

### 3.2.2. Determination of a suitable ANFIS model

The final architecture of the ANFIS model was established by obtaining a minimum error, maximum  $R^2$ , using *gbellmf* and *gaussmf* as best MFs. Table 2 presents the RMSE and  $R^2$  values of these ANFIS models. *Gaussmf* with 3 MFs was selected due to better performance.

**Table 2.** Best Results of ANFIS Models

ANFIS structure		Model performance	
MFs	N	RMSE	$R^2$
<i>gbellmf</i>	2 2 2 2 2 2	0.0215	0.341
	3 3 3 3 3 3	0.0093	0.863
<i>gaussmf</i>	2 2 2 2 2 2	0.0196	0.462
	3 3 3 3 3 3	0.0092	0.867

MFs: membership function type, N: number of membership functions.

### 3.2.3. Prediction Results and Discussion

The ANN and ANFIS model predictions evaluated based on RMSE, MAE and  $R^2$  values (Table 3). RMSE and  $R^2$  values provided information on general error ranges, while MAE value estimated the distribution of errors between model predictions and target values [51]. The good fit between measured and predicted values is improbable to occur, would have RMSE = 0 and  $R^2 = 1$  [52].

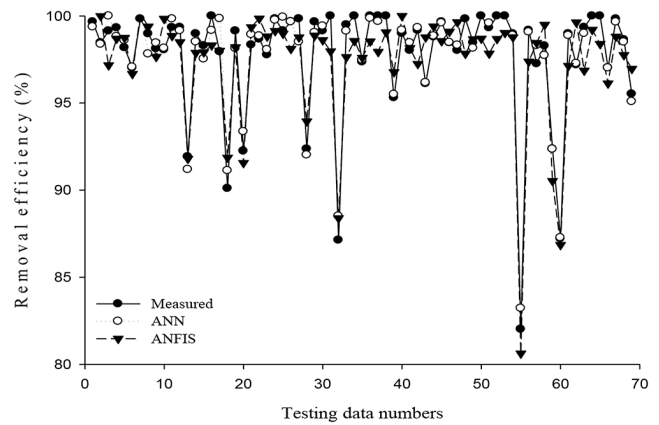
**Table 3.** Proposed ANN and ANFIS Models Performance Criteria

Model	Data	Performance criteria		
		RMSE	MAE	$R^2$
ANN	Train	0.00499	0.00313	0.969
	Validation	0.00618	0.00294	0.948
	Test	0.00556	0.00163	0.973
ANFIS	Train	0.00716	0.00448	0.931
	Validation/checking	0.00783	0.00437	0.895
	Test	0.00924	0.00493	0.867

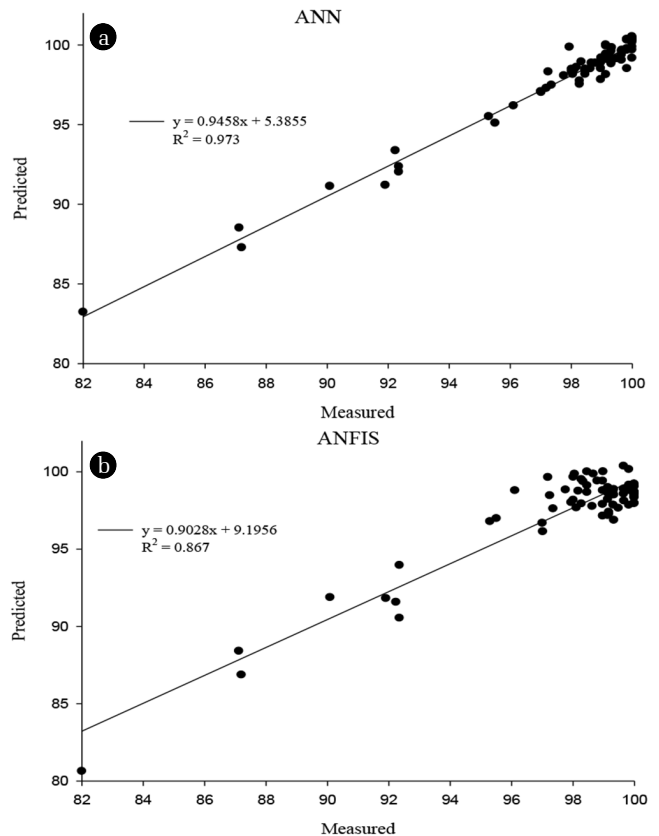
### 3.3. Comparison of ANN and ANFIS Results

Fig. 2 compares experimental data and predicted results of ANN and ANFIS models. This comparison depicts that ANN predictions are close to the experimentally measured results; thus, ANN predictions are relatively better than ANFIS model results. The consistency between the ANN predictions and experimentally measured results for various cases increased the reliability of the proposed ANN model for the prediction of PIMs Cr(VI) removal efficiency. Collectively, the results indicate that a well-trained ANN model can be used to predict removal efficiency without any empirical study that acquires much time and high experimental cost.

The proposed ANN and ANFIS models were assessed by comparing predicted results with experimental results through an independent set of data as presented in Fig. 3. It shows that dots observed well distributed around  $X = Y$  line in a narrow area in the case of ANN model followed by ANFIS. The value of coefficient of determination was  $R^2 = 0.973$  for the line plotted using experimental and predicted data (testing data) for ANN and  $R^2 = 0.867$  for ANFIS model, indicated the reliability of the ANN model.



**Fig. 2.** Comparison of the measured, ANN and ANFIS predicted results of testing dataset.



**Fig. 3.** Comparison of experimental and predicted results of ANN and ANFIS testing dataset.

### 3.4. SA

In SA proposed ANN model results were used. Plus one by one; leave one out, and percentage contribution techniques were employed, and the results presented in Tables S1, S2, and S3, respectively. SA demonstrated that four operating parameters including carrier type; time; film thickness; and plasticizer type are more important than carrier rate and plasticizer rate.

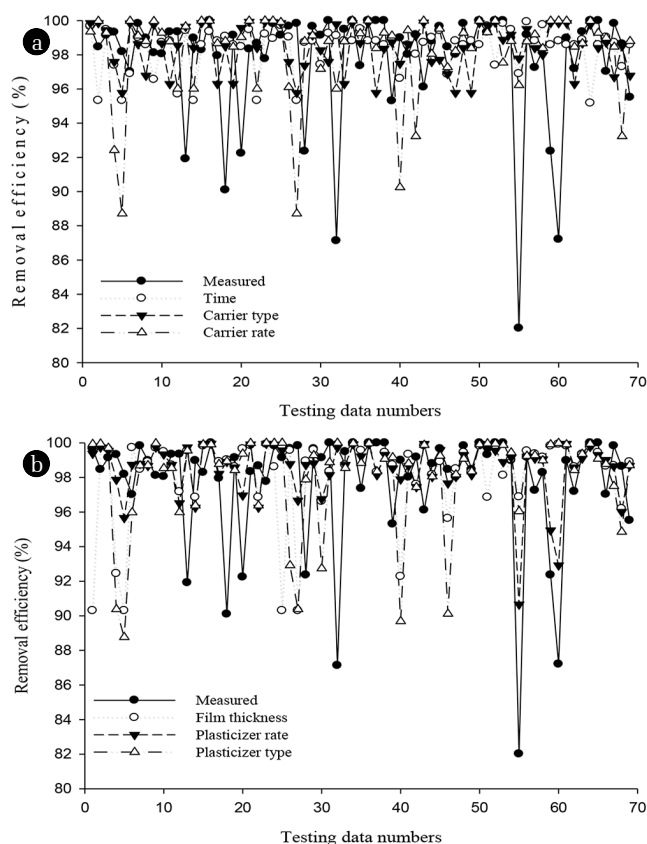


**Fig. 4.** Sensitivity analysis of testing data by using leave one out approach (a) removal efficiency while time; carrier type; and carrier rate left out (b) film thickness; plasticizer rate; and plasticizer type left out one by one.

The study of plus one by one technique does not indicate clearly which parameter is more influential, although it is giving a direction about best data set. Results of this approach as described in Table S1 indicated that a-b-c-d set gave values of  $R^2$  up to 80%. The leave-one-out approach provided similar results as plus one by one technique. Leave-one-out technique confirmed that there are four major influencing parameters namely carrier type; time; film thickness; and plasticizer type as depicted in Table S2.

Moreover, percentage contribution analysis supported the results obtained by the other two methods. This analysis provided further support that carrier type; time; film thickness along with plasticizer type are significant operating parameters than carrier rate and plasticizer rate as presented in Table S3. Fig. 4(a) and (b), compares measured (experimental) versus predicted removal efficiency that computed by using leave one out approach. According to data provided in Table S1, S2 and S3 and graphical presentation in Fig. 4(a) and (b), carrier rate and plasticizer rate have no significant effect on PIMs Cr(VI) removal efficiency.

## 4. Conclusions

The ANN model successfully traced the non-linear behavior of

Cr(VI) removal efficiency versus the time; film thickness; plasticizer type and rate; carrier type and rate of PIMs with low relative percentage error. The predictive capability of the ANN model ( $R^2 = 0.973$ ) was better when compared with ANFIS ( $R^2 = 0.867$ ) model. Hence, the proposed ANN model has confirmed to be an adequate interpolation tool to predict Cr(VI) removal efficiency of PIMs as compared to the ANFIS model. However, investigation of ANFIS model also demonstrates that fuzzy network modeling offers a strong potential to predict PIMs removal efficiency of Cr(VI) at an optimum level. SA proved that carrier type; time; film thickness; and plasticizer type were significant operating parameters having 33.61%, 26.85%, 21.07% and 8.917% contributions, respectively.

## Acknowledgments

We are thankful for the financial support provided by the Scientific and Technological Research Council of Turkey (TÜBİTAK), Grant No: TBAG-112T806.

## References

1. Pavithra KG, Jaikumar V, Kumar PS, Sundarrajan P. A review on cleaner strategies for chromium industrial wastewater: Present research and future perspective. *J. Clean. Prod.* 2019;228:580-593.
2. Mishra S, Bharagava RN, More N, et al. Heavy metal contamination: An alarming threat to environment and human health. *Environ. Biotechnol.* 2019;103-125.
3. Peng W, Li H, Liu Y, Song S. A review on heavy metal ions adsorption from water by graphene oxide and its composites. *J. Mol. Liq.* 2017;230:496-504.
4. Carolin CF, Kumar PS, Saravanan A, Joshiba GJ, Naushad M. Efficient techniques for the removal of toxic heavy metals from aquatic environment: A review. *J. Environ. Chem. Eng.* 2017;5:2782-2799.
5. Bankar A, Nagaraja G. Recent trends in biosorption of heavy metals by Actinobacteria. In: *New and Future Developments in Microbial Biotechnology and Bioengineering*. Amsterdam: Elsevier; 2018. p. 257-275.
6. Kumar P, Pournara A, Kim K-H, Bansal V, Rapti S, Manos MJ. Metal-organic frameworks: Challenges and opportunities for ion-exchange/sorption applications. *Prog. Mater. Sci.* 2017;86:25-74.
7. Abdullah N, Yusof N, Lau WJ, Jaafar J, Ismail AF. Recent trends of heavy metal removal from water/wastewater by membrane technologies. *J. Ind. Eng. Chem.* 2019;76:17-38.
8. Ebbers B, Ottosen L, Jensen PE. Electrodialytic treatment of municipal wastewater and sludge for the removal of heavy metals and recovery of phosphorus. *Electrochim. Acta.* 2015;181:90-99.
9. Shahrin S, Lau WJ, Kartohardjono S, et al. Development of adsorptive ultrafiltration membranes for heavy metal removal. In: *Advanced nanomaterials for membrane synthesis and its applications*. Amsterdam: Elsevier; 2019. p. 1-22.
10. Chen M, Shafer-Peltier K, Randtke SJ, Peltier E. Competitive

- association of cations with poly (sodium 4-styrenesulfonate)(PSS) and heavy metal removal from water by PSS-assisted ultrafiltration. *Chem. Eng. J.* 2018;344:15-164.
11. Tran T-K, Chiu K-F, Lin C-Y, Leu H-J. Electrochemical treatment of wastewater: Selectivity of the heavy metals removal process. *Int. J. Hydrogen Energ.* 2017;42:27741-27748.
  12. Pabby AK, Rizvi SSH, Sastre AM. Handbook of membrane separations chemical, pharmaceutical, food, and biotechnological applications. Vol. 1. Boca Raton: CRC Press; 2008.
  13. Han D, Row KH. Recent applications of ionic liquids in separation technology. *Molecules* 2010;15:2405-2426.
  14. Park Y-S, Chon T-S, Kwak I-S, Lek S. Hierarchical community classification and assessment of aquatic ecosystems using artificial neural networks. *Sci. Total Environ.* 2004;327:105-122.
  15. Shetty GR, Chellam S. Predicting membrane fouling during municipal drinking water nanofiltration using artificial neural networks. *J. Membr. Sci.* 2003;217:69-86.
  16. Belanche L, Valdés JJ, Comas J, Roda IR, Poch M. Prediction of the bulking phenomenon in wastewater treatment plants. *Artif. Intell. Eng.* 2000;14:307-317.
  17. Gholamreza A, Afshin M-D, Shiva HA, Nasrin R. Application of artificial neural networks to predict total dissolved solids in the river Zayanderud, Iran. *Environ. Eng. Res.* 2016;21: 333-340.
  18. Abraham A. Adaptation of fuzzy inference system using neural learning. In: Nedjah N, Macedo Mourelle L, eds. *Fuzzy Systems Engineering*. Berlin: Springer; 2005. p. 53-83.
  19. Elmolla ES, Chaudhuri M, Eltoukhy MM. The use of artificial neural network (ANN) for modeling of COD removal from antibiotic aqueous solution by the Fenton process. *J. Hazard. Mater.* 2010;179:127-134.
  20. Cote M, Grandjean B, Lessard P, Thibault J. Dynamic modelling of the activated sludge process: Improving prediction using neural networks. *Water Res.* 1995;29:995-1004.
  21. Gontarski C, Rodrigues P. Simulation of an industrial wastewater treatment plant using artificial neural networks. *Comput. Chem. Eng.* 2000;24:1719-1723.
  22. B. Eren, M. Yaqub, and V. Eyupoglu. A comparative study of artificial neural network models for the prediction of Cd removal efficiency of PIMs. *Desalin. Water Treat.* 2019;143: 48-58.
  23. Kardam A, Raj KR, Arora JK, Srivastava S. ANN modeling on predictions of biosorption efficiency of zeolites for the removal of Cr(III) and Cr(VI) from waste water. *Int. J. Math. Trends Technol.* 2011;2:23-29.
  24. Kabuba J, Mulaba-bafubandi AF. The use of Neural Network for modeling of copper removal from aqueous solution by the ion-exchange process. In: *International Conference on Mining, Mineral Processing and Metallurgical Engineering (ICMMME' 2013)*; 15-16 April 2013; Johannesburg. p. 131-135.
  25. Lingamdinne LP, Koduru JR, Chang Y-Y, Karri RR. Process optimization and adsorption modeling of Pb(II) on nickel ferri-oxide-reduced graphene oxide nano-composite. *J. Mol. Liq.* 2018;250:202-211.
  26. Karri RR, Sahu JN. Modeling and optimization by particle swarm embedded neural network for adsorption of zinc(II) by palm kernel shell based activated carbon from aqueous environment. *J. Environ. Manage.* 2018;206:178-191.
  27. Madhloom HM. Modeling of Copper removal from simulated wastewater by adsorption on to fungal biomass using artificial neural network. *Glob. J. Adv. Pure Appl. Sci.* 2015;5:35-44.
  28. Kardam A, Raj KR, Arora JK, Srivastava MM, Srivastava S. Artificial neural network modeling for sorption of cadmium from aqueous system by shelled moringa oleifera seed powder as an agricultural waste. *J. Water Resour. Prot.* 2010;2:339-344.
  29. Fan M, Hu J, Cao R, Xiong K, Wei X. Modeling and prediction of copper removal from aqueous solutions by nZVI/rGO magnetic nanocomposites using ANN-GA and ANN-PSO. *Sci. Rep.* 2017;7:18040.
  30. Turgut HI, Eyupoglu V, Kumbasar RA, Sisman I. Alkyl chain length dependent Cr(VI) transport by polymer inclusion membrane using room temperature ionic liquids as carrier and PVDF-co-HFP as polymer matrix. *Sep. Purif. Technol.* 2017;175: 406-417.
  31. Eyupoglu V. Alkyl chain structure-dependent separation of Cr(VI) from acidic solutions containing various metal ions using liquid-liquid solvent extraction by butyl-based imidazolium bromide salts. *Desal. Water Treat.* 2016;57:17774-17789.
  32. Dombaycı ÖA. The prediction of heating energy consumption in a model house by using artificial neural networks in Denizli-Turkey. *Adv. Eng. Softw.* 2010;41:141-147.
  33. Sgarlata C, Arena G, Longo E, Zhang D, Yang Y, Bartsch RA. Heavy metal separation with polymer inclusion membranes. *J. Membr. Sci.* 2008;323:444-451.
  34. Sug H. The effect of training set size for the performance of neural networks of classification. *WSEAS Trans. Comput.* 2010;9:1297-1306.
  35. Leardi R. Nature-inspired methods in chemometrics: Genetic algorithms and artificial neural networks. Amsterdam: Elsevier; 2003.
  36. Agatonovic-Kustrin S, Beresford R. Basic concepts of artificial neural network (ANN) modeling and its application in pharmaceutical research. *J. Pharm. Biomed. Anal.* 2000;22:717-727.
  37. Singh G, Kandasamy J, Shon HK, Cho J. Measuring treatment effectiveness of urban wetland using hybrid water quality - Artificial neural network (ANN) model. *Desal. Water Treat.* 2011;32:284-290.
  38. Gunaydin O, Gokoglu A, Fener M. Prediction of artificial soil's unconfined compression strength test using statistical analyses and artificial neural networks. *Adv. Eng. Softw.* 2010;41: 1115-1123.
  39. Ikizler SB, Aytekin M, Vekli M, Kocabaş F. Prediction of swelling pressures of expansive soils using artificial neural networks. *Adv. Eng. Softw.* 2010;41:647-655.
  40. Jang JR. ANFIS Adaptive-network-based fuzzy inference system. *IEEE Trans. Syst. Man Cybern.* 1993;23:665-685.
  41. Suparta W, Alhasa KM. Modeling of tropospheric delays using ANFIS. Amsterdam: Springer; 2016.
  42. Dogan E. Reference evapotranspiration estimation using adaptive neuro-fuzzy inference systems. *Irrig. Drain.* 2009;58: 617-628.
  43. Sivanandam SN, Sumathi S, Deepa SN. Introduction to fuzzy logic using MATLAB. Amsterdam: Springer; 2007.
  44. Ismail AY, Ismail R, Darus IZ. Dynamic characterization of

- flexible vibrating structures using adaptive neuro-fuzzy inference system (ANFIS). In: 4th Student Conference on Research and Development; 27-28 June 2006; Shah Alam. p. 156-161.
45. Mohdeb N, Mekideche MR. Determination of the relative magnetic permeability by using an adaptive neuro-fuzzy inference system and 2D-FEM. *Prog. Electromagn. Res.* 2010;22:237-255.
  46. Walia N, Singh H, Sharma A. ANFIS: Adaptive neuro-fuzzy inference system-a survey. *Int. J. Comput. Appl.* 2015;123:32-38.
  47. Selma B, Chouraqui S. Neuro-fuzzy controller to navigate an unmanned vehicle. *SpringerPlus* 2013;2:188.
  48. Siddique R, Aggarwal P, Aggarwal Y. Prediction of compressive strength of self-compacting concrete containing bottom ash using artificial neural networks. *Adv. Eng. Softw.* 2011;42:780-786.
  49. Dogan E, Ates A, Yilmaz EC, Eren B. Application of artificial neural networks to estimate wastewater treatment plant inlet biochemical oxygen demand. *Environ. Prog.* 2008;27:439-446.
  50. Eyoupoglu V, Yaqub M, Eren B. Assessment of neural network training algorithms for the prediction of polymeric inclusion membranes efficiency. *SAÜ Fen Bilim. Enstitüsü Derg.* 2016;20: 533-542.
  51. Eren B, Ileri R, Dogan E, Caglar N, Koyuncu I. Development of artificial neural network for prediction of salt recovery by nanofiltration from textile industry wastewaters. *Desal. Water Treat.* 2012;50:317-328.
  52. Daliakopoulos IN, Coulibaly P, Tsanis IK. Groundwater level forecasting using artificial neural networks. *J. Hydrol.* 2005;309: 229-240.